Investigating Ageing Process of Die Cast Aluminum in Squirrel Cage Rotors Exposed to Heavy-Duty Load Conditions

Constantin Pitis[1,*] and Zaid Al-Chalabi[2]

[1]*Powertech Labs. Inc. Canada*

[2]*ASA Energy Consulting Canada*

Abstract: Most of the applications used in underground mining industries (explosion-proof environment) are performing in heavy-duty load conditions. As a result, standard designs of explosion-proof, water-cooled squirrel cage induction motors (WC-SCIM) equipped with standard designs of die-cast aluminium rotors (DCAR) are exposed to higher than expected rotor bar current values. Site investigations and dynamometer tests confirmed that severe heavy-duty loading induce high thermo-mechanical stresses (TMS) in DCARs. Frequent occurrences of such TMS (superimposed on the rated condition stresses) may bring conductive material (Aluminum) of the rotor bars to its fatigue conditions initiating rotor degradation process with subsequent influence on motor performances with consequent financial losses. The paper uses multidisciplinary techniques to study the ageing process of Die Cast Aluminum in Squirrel Cage Rotors Exposed to Heavy-Duty Load Conditions of a 50 hp SCIM equipped with DCAR. Based on claims regarding performance degradations, the research started with site measurements confirming the adverse heavy-duty load conditions. Statistic-probabilistic methods are used to determine Reliability indicators by using Fault Tree Method (FTM). The mathematical model confirmed the motor reliability and enable detection of weak points of the motor. Thermodynamic calculations are used to assess motor performances and its reliability by estimating air gap reduction and heat transfer to the bearings as the two major consequential effects of the TMS developed within DCAR. Dynamometer tests have been used to replicate the site conditions enabling creation of a mathematical model of thermal stress inside the rotor bars. After specific dynamometer tests a number of rotors have been cut-open to investigate the intimate rotor bar degradation. While there are various methods of detecting failed rotor bars, a Secondary research performed by authors indicate that to date no other research has been undertaken in studying this phenomenon.

Keywords: Aluminum cage rotor, Boucherot slot, Fault Tree, Heavy Duty Load, Induction Motor, Life Assessment, Reliability, Thermal Mechanical Stress.

I. INTRODUCTION

Applications requiring heavy duty load conditions are mostly found in underground mining (explosion-proof environment) and heavy industries. One of typical examples represents the underground cutting coal continuous miner (CM) - cutting and bolting machine, as shown in Figure **1**.

Figure 1: Typical 600 kW underground CM (courtesy of Sandvik Mining – Netherlands).

Explosion proof water-cooled induction motors WC-SCIM employed by such application types are working in special loading, power supply and environment conditions – as being defined by 5 (five) Essentials of Application Engineering [1, 2].

The definition of heavy-duty loading conditions emerged based on direct measurements performed over the years on various underground equipments (as presented in the case study, below). Explosion-proof water-cooled squirrel cage induction motors WC-SCIM are restricted by sizes, working in condition of relatively lax protection systems, with mechanical load being directly connected during starting procedure. The WC-SCIM are required to deliver high values of accelerating torque and have to comply with specific heavy-duty load conditions that are defined by four specific characteristics:

- High load inertia: the motor torque shall exceed the load torque (motors being subject of numerous Direct-On-Line starting conditions and able to sustain forward and reverse startings with cutting rims of continuous miner being engages directly on the coal surface) enabling large acceleration torque values over entire speed-torque curve, yielding high acceleration torque values at low values of run up time;
- Large range of loading: the motor shall perform in a very large range of speed/slip values, including overloading (that may exceed sometime 1.5 full load conditions)

*Address correspondence to this author at the 12388-88th Ave. Surrey, BC V3W 7R7 Canada; Tel: 6042308915; E-mail: Constantin.Pitis@powertechlabs.com

E-ISSN: 2311-8741/17

- Unstable load: the motor has to respond to large range of load disturbances (surge loads due to rocks hardness variability) operating with sharp changes in slip;

- Operational pattern: frequent DOL stop/starting (re-closures), forward and reverse directions, prolonged stall conditions, large variations of load with motor operating at very large slip values with torque values sometime close to the Pull Out Torque values;

The paper undertakes to study Ageing Process of DCAR used for Squirrel Cage Rotors when Exposed to Heavy-Duty Load Conditions

The paper uses multidisciplinary techniques to study the ageing process of Die Cast Aluminum in Squirrel Cage Rotors Exposed to Heavy-Duty Load Conditions occurring in South African mining industry. The research was focused on 50 hp SCIM (gathering arm motor) equipped with DCAR.

Based on customer claims regarding performance degradations, the research started with site measurements confirming the adverse heavy-duty load conditions.

Statistic-probabilistic methods were used to determine Reliability indicators by using Fault Tree Method (FTM). The mathematical model confirmed the values of motor reliability indicators within acceptable accuracy range. Further on the study of mathematical model enabled detection of weak points of the motor design with respect to the heavy duty load conditions.

Thermodynamic calculations were used to assess motor performances and its reliability indicators in condition of air gap reduction and heat transfer to the bearings as the two major consequential effects of the Thermo-Mechanical Stresses (TMS) developed within DCAR. Dynamometer tests have been used to replicate the site conditions enabling creation of a mathematical model of thermal stress inside the rotor bars.

Specific dynamometer tests have been used to simulate the heavy duty load conditions on a number of motors were followed by rotors being cut-open to investigate the intimate rotor bar degradation.

II. SETTING THE PROBLEM

Since early 80's overseas-designed CMs have been imported in South Africa for use in coal mining industry. Their declared rated performance of 40,000 tons of coal cut/month has been totally outrun in RSA, with production figures ranging between 80,000 and 120,000 tons of coal/month; that is because of:

- Coal properties, allowing for higher speed of the coal-cutting process

- Higher speed of the process tempted the user to increase productivity enjoying economic advantages

- Higher productivity enabled attractive export opportunities at competitive price (€ 45…€ 55/ton of coal).

However, after a while, it becomes obvious that some overseas-designed motors powering these CMs not satisfy the harsh South African requirements. The machinery failure rate increased beyond expectations with high financial losses – one example is shown in Table **1**. Statistical data enables financial assessment of a specific motor failure:

- Stoppage time = 14 hours (requiring replacing and commissioning new motor);

- Estimated average production rate/hour at 90,000 tons/month, 720 hours/month ≈ 120 tons/hour;

- Annual average running time 8320 hours/year.

- In the DPC (downtime production costs) all other costs are included @ Euro 50/hour.

Table 1: Financial Losses Generated by Failure of a Specific SCIM

Item	Costs (€)	Financial loss (€)
DPC rate	120 t/h x 50 €/t = 6000 €/h	
DPC loss @ 14h	6000 €/h x 14 h	84,000
Special Labor	80 €/h x 15 h	1,200
Penalties ≈ 30%	84,000 x 0.1	25,200
Logistics	50 €/h x 1.5 x 14 h	1,300
Salaries	40 €/h x 15 h	600
New motor	**57,000**	
New rotor	20,000	22,000
Av. cost repair	Max 65 % of new	38,000
Total losses	Estimative	**172,300**

The total financial losses are about threefold higher than the cost of a new motor (172,300: 57,000 ≈ 3).

Besides the issue of equipment reliability (requiring investigation of root cause of failure) customer was also concerned if repair/replace policy was properly applied.

The paper focuses on a 50 hp gathering arm SCIM (marked by arrows in Figure **1**) which recorded high failure rate with mean time to the first failure of $T_{New,\ 0}$ = 5380 h/y, while on the repaired motors $T_{Repair,\ 0}$ = 3770 h/y resulting in notable negative financial effect on the business.

III. INVESTIGATING RELIABILITY OF A WC-SCIM

Since reliability is the reciprocal of failure, and failure is a random event, the use of probabilistic measures are most appropriate, thus the laws of probability theory shall apply. Multidisciplinary techniques as statistic-probabilistic methods in estimating reliability and thermodynamics calculations must also be correlated.

Mathematical modeling of "fault tree method" (FTM) is used to assess a process or to design a financially competitive product with improved technical performances is currently employed in various fields.

Fault tree analysis is a method of combining various components failure rates, being initially used to analyse the Minuteman Launch Control System [3]. Refined over the years, the method models system' failure of interest called Top Event (**TE**) i.e. equipment failure. The fault tree breaks down **TE** into lower-level events (**LLE**) in terms of failure rate intensities λ_i.

The failure rate intensity can be estimated based on direct recordings of Mean Time between Failures – MTBF indicator:

$$\lambda_i = \frac{1}{MTBF_i}$$

Logic gates show the relationship between LLE and TE. Mathematical model is based on Boolean algebra.

The "OR" gate showed in Figure **2a** express the idea that ANY of several component failures can cause output event i.e. TE = equipment or process failure.

The output event - the failure rate intensity of the WC-SCIM $\mathbf{\Lambda}_o$ is therefore a function of LLE failure rates λ_i and can be calculated as:

$$\Lambda_o = \Sigma\ \lambda_i \text{ [1/hours] units} \quad (1)$$

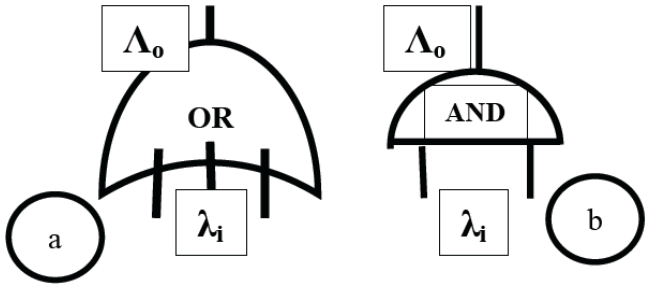

Figure 2: Graphical Description of gate "OR" and gate "AND".

The gate "AND" showed in Figure **2b** express the idea that both (or all) components must fail in order to produce the output event. The output event failure rate $\mathbf{\Lambda}_o$ is therefore a function of LLE failure rates λ_i and can be calculated as:

$$\mathbf{\Lambda}_o = \Pi\ \lambda_i \text{ [1/hours] units} \quad (2)$$

A basic FTM graph, as shown in Figure **3**, was used to analyze reliability indicators for a water-cooled squirrel cage induction motor WC-SCIM.

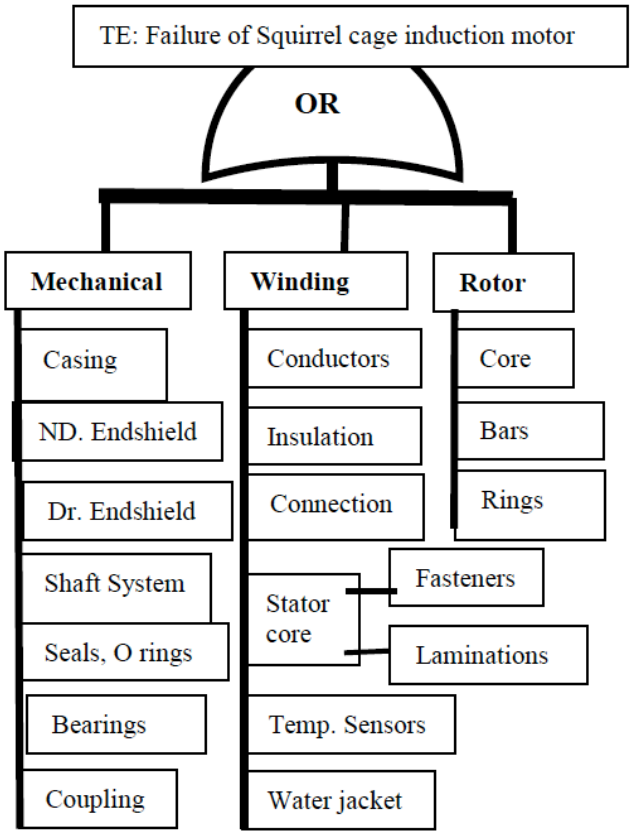

Figure 3: Simplified FTM graph for a typical water-cooled SCIM.

As a method of combining various component failure rates, the fault tree breaks down top event (TE) – that is considered to be WC-SCIM failure, into lower-level events (LLE) as failures of various components.

Mechanical components, winding and rotor failures are considered the first LLE tier connected by "OR" gate, meaning any of them can produce TE.

Under Mechanical, Winding and Rotor LLE, there are second tier of LLE components, but for simplicity, the diagram does not indicate their "AND" and "OR" logical connections.

An initial assumption was to consider the SCIM under study as a product with simple function, while some of the second tier components have reparability function (casing, water jacket, end shields, shaft and coupling, stator' electrical and magnetic circuits).

Rotor assembly was initially considered having reparability function, but further analyze of its reliability indicators conducted to conclusion of reversing such decision.

At the sponsor request an initial estimation of reliability indicators has been performed in early 90's on a 50 hp 4 poles WC-SCIM (equipped with DCAR) driving gathering arms of CM (indicated with arrows in Figure **1**). Its rated data are shown in Table **2**.

Table 2: Rated Data 50 hp WC-SCIM

Power [kW] @ 50 Hz	36.0
Efficiency [%]	87.0
Rated current [A] @ 1000 V	28.6
Starting Torque [Nm]	238
Full-load speed [rpm]	1442
Winding Temp. Rise [°C]	100–110

Statistical data collected over 5 years of the mean time to the first failure (MTBF) for new motors has been analyzed by using FTM with results as shown in Table **3**. Failure intensity rate is expressed in 10^{-6} [hour]$^{-1}$.

Upon analyzing statistical data and conducting preliminary investigations it was found that:

- Mathematical Model (MM) used to create FTM confirmed mean time to the first failure of the new motors $T_{New,\ 0}$ = 5380 h/y, in spite of internal and external protection of the WC-SCIM (RTD 90°C on bearings and 140° C on winding phases, plus overload and thermal current protection)
- Validated FTM was considered as Baseline and used to investigate reliability indicators of the first LLE tier: Mechanical, Winding and Rotor assemblies
- Mechanical system with high value of failure intensity, was found to be attributed to the bearings (with average life value of 0.5 years),
- Analyze of bearing failures found mostly no major number of contamination events, but rather "thermal contamination" (in spite of strictly controlled greasing procedure, correct amount of grease and grease type),
- It was suspected that rotor may evacuate heat energy via shaft into inner ring of the bearing reducing bearing clearance, before RTD installed on the endshield (outer ring) may react with a noticeable time-delay – that could be the time interval when bearing damage may occur,
- It was suspected the rotor thermal expansion may reduce the air gap values which in turn may affect torque availability.

The above suppositions combined with relatively high value of failure intensity rate of the rotors themselves conducted to decision of further investigations of the DCAR used for these motors

IV. SITE INVESTIGATIONS PERFORMED ON DCAR EXPOSED TO HEAVY-DUTY LOAD CONDITIONS

Ideally rotors should have large resistance at standstill that decreases as the speed rises. For this

Table 3: Initial Assessment of Reliability Indicators (90's)

SCIM LLE (Assemblies)	MTBF [hours]	λ_i x 10^{-6} [1/hour]	Estimated $T_{New,\ 0}$	Notes
Mechanical	20,830	48.0	2.5 years	Bearings (?)
Winding	13,310	75.1	1.65 years	Acceptable
Rotor	17,060	62.3	2.1 years	Suspect
SCIM – TE	5,400	185.4	0.65 years	Suspect

Source: FEMCO Mining Motors, FMM072 files

reason, DCAR Boucherot slot types (resembling double cage configuration) are preferred option. In a typical configuration, a leakage slot (l_s) is situated between running and starting cages, as shown in Figure **4**.

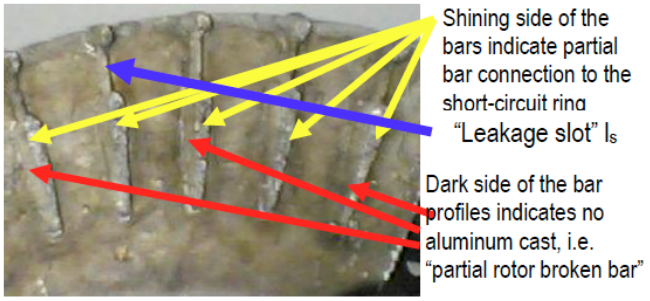

Figure 4: Leakage slot (Boucherot type) connects starting and running cages; due to TMS and quality of cast partial rotor broken bars might be present.

These rotor types require leakage slot (between starting and running cages) yielding large reactance in order to prevent the main flux from missing the running cage bars [4]. During the casting process, an aluminum fillet enters in the leakage slot connecting the upper and the lower parts of the slot. Due to slot configuration the material in the leakage slot fillet is subject of approximate the same induction flux density as the top filament, while the current density performs discontinuities at the both ends of the leakage slot. This could be one of the reasons that, the leakage slot becomes the subject of intense TMS, defining a weak point of the electrical circuit of the rotor [5]. Rotor bar deformations with motor in steady state situations (blocked rotor and various slip values) have been studied and modeled by using Finite Element Method (FEM) [6].

As expected, it was found that the stresses have the greatest values not in the high velocity conditions but on the blocked rotor condition, or at the beginning of the starting: forces about 10 times greater than the integrated centrifugal forces at nominal function. These results confirm previous research that major TMS occurring during heavy-duty loading conditions conducted to rotor degradation [4]. Mechanical tests performed on 1st time repaired motors indicate "supplementary" rotor losses: 1.65 % more than expected (rotor losses are proportional to rotor slip) Table **4**.

Site measurements recorded stator currents on 50 hp, 50 Hz, 1000 V, water-cooled, SCIM proved existence of such load types. A typical example is shown in Figure **5** (blank arrows) depicting repetitive pattern of 5 (five) almost consecutive stresses (loads) on stator (rotor) currents with 1'23" time duration occurring in an interval of 29 minutes, as indicated in Table **5**.

Table 4: Mechanical Tests (Average Values)

Item	Manuf.	Test 1	1st repair
Rated Tq., Nm	238.4 Nm	238.4	239
St. Tq. Cold, Nm	610 Nm	605	585
St. Tq. Hot, Nm	unknown	510	470
St. Tq. Ratio [%]		85 %	80 %
Slip @ 36 kW	58 rpm	60rpm	61rpm
Rotor losses kW	1.508	1.510	1.550

Table 5: Typical Heavy Duty Loading (white Arrows Interval in Figure 5)

#	Time & Duration	Stator Crt	Rotor Crt.
1	1:30, t = 7 sec	91 A	3.2 pu
2	1:39, t = 23 sec	46 A	1.6 pu
3	1:45, t = 16 sec	74 A	2.58 pu
4	1.53, t = 3 sec	93 A	3.25 pu
5	1:59, t = 34 sec	41 A	1.43 pu

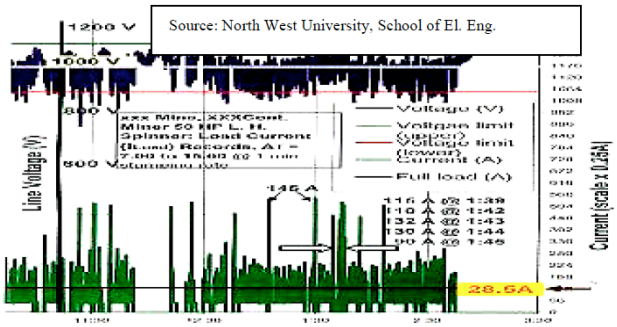

Figure 5: Typical pattern of heavy duty loading (stator current).

It was demonstrated the heavy-duty load conditions generates high values current densities in the leakage slot producing high temperature gradients of 20°C/sec or higher that are superimposed on the temperatures due to rated conditions [5]. Due to short period of occurrence, these consecutive stresses determine a quasi-adiabatic cumulative thermal effect. As a result radial and longitudinal TMS are present in the rotor bars, as shown in Figure **4** and **6**.

V. TESTS PERFORMED

At sponsor request, a series of tests have been performed on 20 new shipments motors and 12 first

time repaired motors (Figure **7**). Speed – torque curve has been investigated (figure 8) and found the rotor not being "D" type design. Other tests performed: heat run test recording and confirming rated values and temperature rise of different components and cooling agent, overload tests, temperature differential values across drive and non-drive bearings in stabilized hot condition and overload, starting torque and current in cold and hot condition.

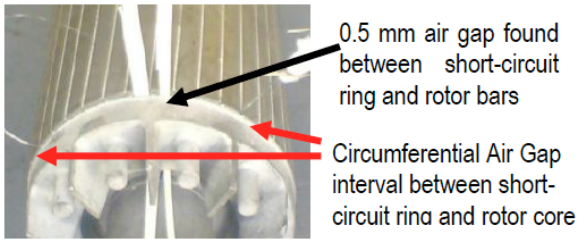

Figure 6: Longitudinal TMS superimposed on quality of cast results in detached short-circuit ring (rotor broken bar).

TH1+TH2=	16.2342B	OUT.WAT=	23.2244	CASING=	54.6134	DRIVE=	57.3514
N/DRIVE=	60.4614	AMBNT=	17.6758	I1=	31.3779	I2=	31.0094
I3=	31.7323	V1=	963.48	V2=	961.94	V3=	958.75
TORQ=	237.27	RPM=	1438.32	HZ=	49.9951	COS Q=	0.834603
KVA=	52.240	INPUTKW=	43.600	SLIP=	61.6907	AVE V=	961.39
AVE I=	31.3732	T/RISE=	102.8491	R1=	1.163200	R2=	1.610000
T1=	22.0000	NoLD.I=	13.2000	NoLd.KW=	2.20000	IrFLOSS=	1.78289
CoLOSS=	2.37703	ADDLOSS=	0.189091	A.GAP=	39.440	RD.C.LS=	1.62179
OUTPUT=	37.629	EFF.=	86.305	OUTP.TQ=	35.735	EFF.TQ=	81.961
AX.VIBR=	1.20000	VT.VIBR=	2.10000	HR.VIBR=	2.50000	NDEVIBR=	3.60000
FLOW=	A.000	DIF.T/R=	0.63274	DIF.R/S=	1.35077	DIF.S/T=	-1.95315

Figure 7: Dyno test bench - sample of test records.

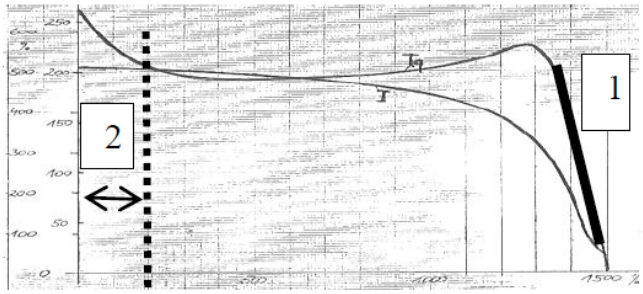

Figure 8: Speed–Torque Curve on new motor (dyno test); motor doesn't have a "D" design rotor!

The following data have been retained for further investigations.

- Thermal equilibrium @ heat run test t ≈ 3.0 h
- Ambient, T_0 = 25 C
- DE bearing T. Rise ΔT_{DE} = 45 C
- NDE bearing T. rise ΔT_{NDE} = 55 C
- Rotor RI^2 losses @ N_{nom}, ΔP_{rotor} = 1.51 kW
- Rotor assembly mass, M = 162 kg
- Stator ID, D_{stator} = 165 mm
- Cold Rotor OD, D_0 = 163.6 mm (cold)
- Air gap cold motor, AG_{cold} = 2 x 0.7 mm

VI. INVESTIGATING ROTOR THERMAL EXPANSION

Rotor thermal expansions resulting in airgap reduction have been studied at full load for new and for a 1st tine repaired motor

Rotor stabilized average temperature (heat run test), $T_{rotor,\ hot}$ = 205 C is obtained from (3)

$$\Delta P_{rotor} \times t = M \times (c = 490\ J/kg\ K) \times T_{rotor,\ hot} \quad (3)$$

Hot Rotor OD, D_{hot} = 164.0 mm is obtained from (4)

$$D = Do\ [1 + [\alpha = 15.7 \exp(-6)] \times \Delta T_{rotor}] = 164.0 \quad (4)$$

Air gap hot motor $AG_{hot} = D_{stator} - D_{hot}$ = 1.0 mm = 2 x 0.5 mm

Air gap reduction: Δ AG = 2 x 0.5 mm or percentagewise: $\varepsilon_{AG} = AG_{hot} / AG_{cold} \approx 72\ \%$

The results of mechanical tests are shown in Table **5**. Starting torque values in hot conditions are about 80%...85% of those in cold conditions; pull-out torque values are reduced at the same ratio.

The "supplementary" increase of 1.65 % more than expected rotor losses after 1st repair (rotor losses are proportional to rotor slip) was found to be due to rotor degradation. That was confirmed by forensic reports on two DCARs being cut and investigated (Figure **4** and **6**). The difference between mechanical performances of new and 1st time repaired motors indicates:

- Rotor degradation at the level of rotor bars and shortcircuit rings in an working interval of 5380h
- Rotor losses increased above those due to slip, with higher heat energy
- Notable air gap reduction reduces torque values "dropping" the speed-torque curve, resulting in lower available torque values

- The motor running interval tends to move from stable interval (1) = 1500…1300 rpm to large slip values in interval (2) = 0…200 rpm as dash-marked on Figure **8** where high values of TMS are present [5, 6].

VII. INVESTIGATING HEAT TRANSMISSION FROM ROTOR TO BEARING AND CLEARANCE REDUCTION

The motor is equipped with 2 x 6311 C3 bearings with d = 55 mm, D = 120 mm, B = 29 mm, ball radius r = 0.011 m, mass m = 1.35 kg, average C3 clearance S @ 25 °C = 60 μm, specific heat C = 0.49 kJ/kg °C, thermal conductivities (bearing – K_B = 0.006 kJ/mm sec °C, shaft – K_S = 0.060 kJ/mm sec °C), linear expansion coefficient λ = 15.7 exp (-6) [7]. The NDE bearing is positioned at 240 mm from the rotor center, DE bearing positioned at 250 mm from the rotor center and shaft to thermistor x = 275 mm (Figure **9**). Two RTDs have been installed in points "1" (outer race) and "2" (inner race) monitoring the temperature gradient (Figure **10**).

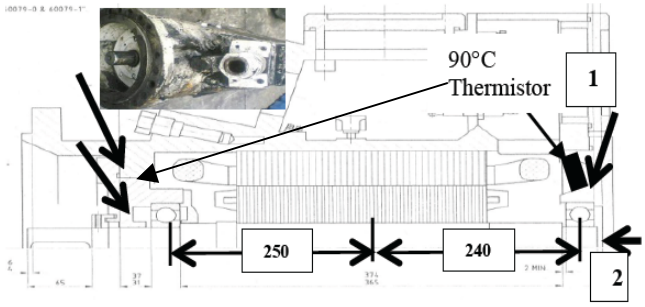

Figure 9: Cross section of 50 hp motor.

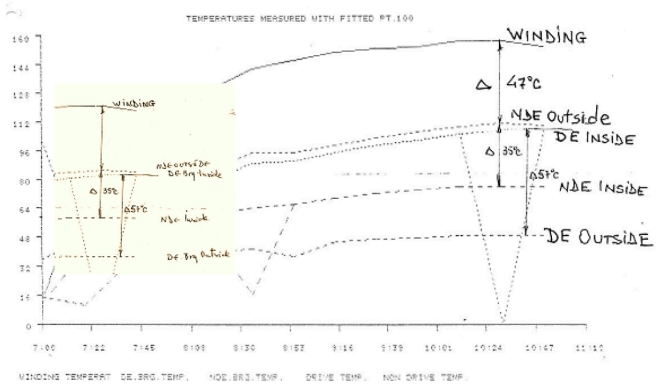

Figure 10: Temperature records and temperature differential values across drive bearings (51 C) and non-drive bearings (35 C) during load condition (enlarged detail on the left hand medallion).

At thermal equilibrium (ΔT_{NDE} = 55°C) the NDE bearing absorbed 2.22% of the rotor heat (3) keeping same clearance

$H_{B,\ Stab}$ = 1.35 x 0.49 x 55 = 36 kJ = 0.0101 kWh = 0.0222 of (ΔP_{rotor} x t) (5)

A steady 36 kW load has been applied when SCIM temperatures were stable at: NDE = 65°C, Winding = 80°C. The RTD installed in close proximity of 90°C thermistor start reacting after about 25 minutes (Figure **11**).

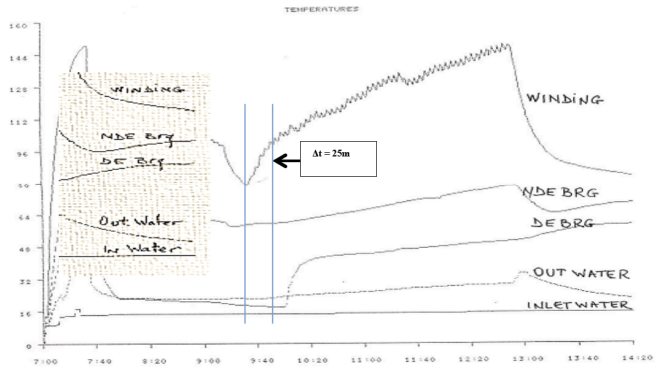

Figure 11: Temperatures evolution during simulation of heavy-duty load on dyno (enlarged detail on the left hand medallion).

Heat transferred to NDE Bearing is $H_{NDE} = \Delta P_{rotor}$ x t x 0.0222 = 1.51 x 0.75 x 0.0222 = 0.0251 kWh = 90.36 kJ

Time duration "t" of transferring heat between Rotor and NDE Bearing Inner ring is:

$$Q_{Transfer} = K\ x\ Area\ x\ \frac{\Delta T}{L}\ x\ t \quad (6)$$

Thus for time duration from rotor to point "2" is $t_{R,2}$ ≈ 3.5 min, while time duration from point "2" to thermistor is $t_{2,Th}$ ≈ 20 min. Total calculated time transfer is Δt = 23.5 min is confirmed by experiment indicating Δt ≈ 25 min (Figure **11**).

The possibility of clearance reduction of the bearings is estimated using thermal resistance R_{BRG} to determine Heat Transfer rate □, which will enable estimation of time duration to transfer the heat via NDE Bearing. It was demonstrated the quasi-adiabatic process of inner ring dilatation could reduce to zero the bearing clearance.

Thermal resistance of the bearing [8] is obtained by applying: $R_{BRG} = \frac{ln^{D}/_{d}}{2\ \Pi\ r\ K}$

Where ln (D/d) = 0.78, r = 0.011 m, K = 46.6 W/m °C

The value of R_{BRG} = 0.242 °C/W is used to estimate Heat Transfer rate □ = (ΔT_{NDE} = 55°C) / R_{BRG} = 145 J/sec.

The time duration to transfer the heat via NDE Bearing is therefore;

$t_{NDE,transfer} = (H_{NDE} / \bar{Q}) = 90360 \text{ J} / 145 = 623 \text{ sec} = 10.4 \text{ min}$

During this time due to thermal expansion, the inner ring will increase the sizes with consequent reduction of clearance: $\Delta S_T = d - d_0 = d_0 \times \lambda \times \Delta T_{NDE} = 55 \times 15.7 \exp(-6) \times 35 = 0.030$ mm = 30 μm, for about 10.4 minutes (in a quasi-adiabatic process type). The operating clearance [9] is $S_{OP} = S - \Delta S_F - \Delta S_T$;

If reduction in radial internal clearance due to fit ΔS_F reaches 30 μm (due to manufacturing interference fit or just fitting itself, the available clearance ($S - \Delta S_T$) = 30 μm could be reduced to ZERO without thermistor's protection be activated, with consequential bearing damage. During motor frequent re-start in the first 10 minutes running condition the bearing could be overheated (and possible collapsed) as a result of an additional thermal shock at motor re-start superimposed on the existent "hot" condition.

CONCLUSIONS

Comprehensive mechanical and thermodynamic tests, together with mathematical simulations proved that for specific applications some standard designs of explosion-proof, water-cooled WC-SCIM equipped with DCAR are exposed to higher than expected Thermo-Mechanical Stresses (TMS).

It was demonstrated that standard designs of explosion-proof, water-cooled squirrel cage induction motors (WC-SCIM) equipped with standard die-cast aluminium rotors (DCAR) are exposed to higher than expected rotor bar current values. Site investigations and dynamometer tests confirmed that severe heavy-duty loading induce high thermo-mechanical stresses (TMS) in DCARs.

Frequent occurrences of such TMS (superimposed on the rated condition stresses) may bring conductive material (Aluminum) of the rotor bars to its fatigue conditions initiating rotor degradation process with subsequent influence on motor performances with consequent financial losses.

As a result a new type of Mixed Conductivity Fabricated Rotor [10] has been undertaken. This topic is subject of another paper.

The authors gratefully acknowledges financial and logistic support of FEMCO Mining Motors, CUSTOM Electric Motors, North West University Potchefstroom Mechanical Dept and Sandvik South Africa who have help them initiating and completing this project.

REFERENCES

[1] Pitis C. The fundamentals and practice of essentials of application engineering concept" EESD15 – The Seventh International Conference on Engineering Education for Sustainable Development, June 2015, https://open.library.ubc.ca/cIRcle/collections/52657/items/1.0064719.

[2] C. Pitis, "Using essentials of application engineering concept for designing industrial system drives" EESD15 – The Seventh International Conference on Engineering Education for Sustainable Development, June 2015, https://open.library.ubc.ca/cIRcle/collections/52657/items/1.0064716.

[3] Schweitzer, EO. Reliability Analysis of Transmission Protection using Fault tree Methods. Schweitzer Engineering Labs, Inc, Pullman, WA, USA 1997.

[4] Alger PL. Induction Machines – Their Behavior and Uses, 2nd Edition, Gordon & Breach Science Publishers, NY USA, pp. 261...268.

[5] Pitis C. Thermo-Mechanical Stresses of the Squirrel Cage Rotors in Adverse Load Conditions. 28th Electrical Insulation Conference, IEEE – ISEI Vancouver 20 08, http://irispower.brinkster.net/ IEEE - Explorer http://ewh.ieee.org/conf/isei

[6] Jun C. Alain Nicolas. "Analysis of the mechanical stresses on a squirrel cage induction motor by the finite element method". IEEE Transactions on Magnetics, Institute of Electrical and Electronics Engineers, 1999, 35 (3 Part 1), pp.1282-1285. <hal-00141539> HAL Id: hal-00141539, https://hal.archives-ouvertes.fr/hal-00141539

[7] Mitton RG. HEAT, J.M.Dent & Sons Ltd, London, 1957, pp 252…277.

[8] Isert S. Heat Transfer Through A Rotating Ball Bearing at low angular velocities. Thesis, Utah State University, Logan, 2011, http://digitalcommons.usu.edu/cgi/viewcontent.cgi?article=1095&context=gradreports

[9] Schaeffler, Medias Professional FAG Rolling Bearings, http://medias.ina.com/medias/en!hp.tg.cat/tg_hr*ST4_102440715.

[10] Pitis CD, van Rensburg J, Kleingeld M and Mathews E. A new approach to the efficiency concept in South African Industry. Journal of Energy in Southern Africa, Proceedings, Vol. 18, Number 1, February 2007, Cape Town, South Africa, pp 51–63. http://www.erc.uct.ac.za/sites/default/files/image_tool/images/119/jesa/18-1jesa-pitis.pdf

Received on 31-05-2017 Accepted on 24-07-2017 Published on 28-12-2017

DOI: https://doi.org/10.12974/2311-8741.2017.05.02.2